AD_____

GRANT NUMBER DAMD17-94-J-4242

TITLE: Electrically Mediated Trauma Repair

PRINCIPAL INVESTIGATOR: Richard B. Borgens, Ph.D.

CONTRACTING ORGANIZATION: Purdue Research Foundation
West Lafayette, Indiana 47907

REPORT DATE: September 1997

TYPE OF REPORT: Annual

PREPARED FOR: Commander
U.S. Army Medical Research and Materiel Command
Fort Detrick, Maryland 21702-5012

REPORT DOCUMENTATION PAGE

Form Approved
OMB No. 0704-0188

1. AGENCY USE ONLY *(Leave blank)*	2. REPORT DATE	3. REPORT TYPE AND DATES COVERED
	September 1997	Annual (22 Aug 96 - 21 Aug 97)

4. TITLE AND SUBTITLE
Electrically Mediated Trauma Repair

5. FUNDING NUMBERS
DAMD17-94-J-4242

6. AUTHOR(S)
Borgens, Richard B., Ph.D.

7. PERFORMING ORGANIZATION NAME(S) AND ADDRESS(ES)
Purdue Research Foundation
West Lafayette, Indiana 47907

8. PERFORMING ORGANIZATION REPORT NUMBER

9. SPONSORING / MONITORING AGENCY NAME(S) AND ADDRESS(ES)
U.S. Army Medical Research and Materiel Command
Fort Detrick, Maryland 21702-5012

10. SPONSORING / MONITORING AGENCY REPORT NUMBER

11. SUPPLEMENTARY NOTES

12a. DISTRIBUTION / AVAILABILITY STATEMENT
Approved for public release; distribution unlimited

12b. DISTRIBUTION CODE

13. ABSTRACT *(Maximum 200 words)*

In this contract year, we have finished development of a quantitative three dimensional computer assisted morphometric technique used for the evaluation of spinal cord pathology. This has been applied to an evaluation of the effect of applied electric fields (which produce functional recovery) on the robust inflammatory reaction produced by CNS injury. Though preliminary data suggested an interaction, this did not hold up following a thorough examination with our more rigorous methods. A direct effect of DC fields on damaged axons was demonstrated in the first year of this contract, however, it does not appear that activated phagocytes are a secondary target. This contract year has seen two other important advancements: 1) We have proven that the applied field in combination with another known facilitator of nerve regeneration (polymeric guidance channels) can induce and direct robust mammalian spinal axon regeneration, and 2) acute rescue of nerve fibers doomed to separate and become nonfunctional is also possible - providing larger numbers of fibers for ancillary restorative techniques. This is accomplished through the application of artificial membrane polymers that can fuse, seal, and even permit nerve conduction across the lesion.

14. SUBJECT TERMS	15. NUMBER OF PAGES
Neurotrauma, Spinal Cord, Paraplegia	34
	16. PRICE CODE

17. SECURITY CLASSIFICATION OF REPORT	18. SECURITY CLASSIFICATION OF THIS PAGE	19. SECURITY CLASSIFICATION OF ABSTRACT	20. LIMITATION OF ABSTRACT
Unclassified	Unclassified	Unclassified	Unlimited

FOREWORD

Opinions, interpretations, conclusions and recommendations are those of the author and are not necessarily endorsed by the U.S. Army.

____ Where copyrighted material is quoted, permission has been obtained to use such material.

____ Where material from documents designated for limited distribution is quoted, permission has been obtained to use the material.

____ Citations of commercial organizations and trade names in this report do not constitute an official Department of Army endorsement or approval of the products or services of these organizations.

____ In conducting research using animals, the investigator(s) adhered to the "Guide for the Care and Use of Laboratory Animals," prepared by the Committee on Care and Use of Laboratory Animals of the Institute of Laboratory Resources, National Research Council (NIH Publication No. 86-23, Revised 1985).

____ For the protection of human subjects, the investigator(s) adhered to policies of applicable Federal Law 45 CFR 46.

____ In conducting research utilizing recombinant DNA technology, the investigator(s) adhered to current guidelines promulgated by the National Institutes of Health.

____ In the conduct of research utilizing recombinant DNA, the investigator(s) adhered to the NIH Guidelines for Research Involving Recombinant DNA Molecules.

____ In the conduct of research involving hazardous organisms, the investigator(s) adhered to the CDC-NIH Guide for Biosafety in Microbiological and Biomedical Laboratories.

PI - Signature Date

Table of Contents

I. Introduction

Certainly the most intractable, but survivable, wartime injury is trauma to the Central Nervous System (CNS). Blunt force contusion to, (and less commonly, laceration of), the Brain and Spinal Cord produce catastrophic loss of function. These deficits are not able to be reversed by present medical technology. Novel medical interventions that can be applied very early in the CNS injury process to rescue function have been particularly emphasized in the US Army Science and Technology Master Plan (1996). This rescue can be theoretically accomplished by acute applications that boost the healing potential of the CNS through mechanisms of neuronal regeneration, and/or reduce the "delayed" or "secondary" injury processes that are initiated at the moment of insult -- but continue to destroy CNS parenchyma subsequently. One such intervention, the use of applied electrical fields, is the subject of this active investigation. Modern bioelectronics has made it possible to apply steady, controlled, gradients of extracellular voltage to target areas within the spinal cord. Moreover, these techniques are noninvasive (to the spinal cord itself). There is now a substantial, modern literature, that demonstrates exogenous extracellular voltages can affect regeneration, guidance of growing neurites, and the preservation of damaged white matter (reviewed by Borgens 1989, 1992, and Borgens and Bohnert 1997; see also the Introductions to the original proposal and to the first annual report of August, 1995).

This contract explores the development of this technology on two fronts: 1.) To test a slowly oscillating DC electric field applied to *clinical cases* of acute, neurologically complete, paraplegia in a veterinary model (Borgens et al 1993). Also, 2.) To investigate mechanisms of action and target cells in a *laboratory model of spinal injury* (Borgens et al 1986 a, b, 1987, 1990) using adult guinea pigs.

The body to this annual report will begin with a reporting of completed laboratory work discussed as preliminary findings in last years report. A brief introduction to these parts of the work plan is provided for continuity. New Methods and Preliminary Findings will follow. We will save an accounting of all work completed in this 3 year work plan for the final report due next year as many of the investigations described in the preceding annual reports have now been completed, submitted for publication, or published, and the canine clinical trial is still ongoing.

II. Body

1.) Quantitative Evaluation of Macrophage invasion of the Subacute Spinal Cord Injury by Two and Three Dimensional Computer Morphometry.

In last year's report we provided much detail on the background, methods, and animal use during the development of a computer based morphometric investigation of monoclonal antibody (ED 1) labeled activated macrophages that invade the acute spinal injury. We further detailed the methods used to verify the computer assisted counting of macrophages and the ability to graphically evaluate the injury by novel three dimensional shape and volume reconstruction of histological materials. All of this material was subsequently submitted to the Journal of Neurological Sciences and has recently been accepted for publication. This new method was applied to an investigation of macrophage responses *in vivo* , to applied electric fields in the guinea pig spinal injury model (to be updated in the next section, below).

Here we further add both rationale and methodological development of this quantitative computer based technology that was not described in our last report -- but was included in our recent publication. This addition gave us the ability to accurately determine both surface area and volume (in mm^2) of any structure, or imbedded structure, included in the graphic reconstruction of histology.

Method and Rationale

The algorithms used in this study construct planar contours of cord, lesion, and cysts as images via a process of segmentation. The constructed planar contours are polygons. The task is to construct surface meshes which interpolate the contours on two adjacent histological sections. The 3-D surface construction from planar contours requires a solution to *correspondence, tiling,* and *branching* problems.

The *correspondence* problem involves finding the correct connections between the contours of adjacent histological sections. *Tiling* refers to the use of boundaries to triangulate the strip lying between contours of adjacent sections into triangles. A *branching* problem occurs when a contour in one section may correspond to more than one contour in an adjacent section. The possibility of branching significantly complicates the task of tiling.

We approach the solution to all of these problems simultaneously (Bajaj et al 1996). This is accomplished by imposing a set of three mathematical constraints on the reconstructed surface and then deriving precise correspondence and tiling rules from these constraints. The constraints ensure that the regions tiled by these rules obey physical constructs and have a natural appearance.

Once a surface (wire frame or tiled mesh) is constructed, quantitative interrogation of the reconstruction to provide precise surface areas and volumes can be accomplished. The surface area of the 3-D image is simply the sum of all triangles. If the tiling process does not develop any untiled region, the reconstructed shape is a prismatoid that is a triangular tiled region between two parallel contours. If the reconstructed shape is not a prismatoid, it can be reduced into prismatoids. A prismatoid is a polyhedron that consists of two planar contours in parallel planes and lateral triangles. The three vertices of each lateral triangle must be the vertices of both planar contours. The volume of a prismatoid is calculated as $V = \frac{h}{6} (B_1 + 4M + B_2)$ where B_1 is the area of the lower base, B_2 is the area of the upper base, M is the area of the midsection joining the bases and h is the separation between contours. With n parallel slices of contours equally spread, the composite volume computation results in: $V^1 = \frac{h}{6} (B_1 + 4\sum_{1}^{n-1} Mi + 2\sum_{2}^{n-1} Bi + Bn)$.

These novel methods provided the quantitative abilities of our custom software to both compare and verify the 2D morphometry as well as older methods found in the literature to estimate spinal lesion volumes and surface areas. These comparisons are provided in table I.

2.) Macrophage Density at Spinal Lesion is Unaffected by the Applied Voltage Gradient

Introduction

In the last annual report, we provided preliminary data suggesting that both macrophage numbers (density /mm^2 of lesion) and the associated amount of cavitation produced by phagocytosis was reduced by the applied voltage gradient (300 - 400 uV/mm^2). The rationale for this evaluation was described in the original workplan and in last year's reports, briefly: Macrophages are known to preferentially migrate towards the anode (+ pole) of an applied electric field (Orida and Feldman

Table 1 Quantification of spinal cord segments, spinal cord lesions, and cysts formation: comparative evaluation using 3-D surface reconstruction, formulaic, and 2-D morphometry.

Rat #	Three Dimensional Morphometry[1]						Comparative Data[2]			
	A	B	C	D	E	F	G	H	I	J
	Cord Volume in mm^3	Cord Surface Area in mm^2	Lesion Volume in mm^3	Lesion Surface Area in mm^2	Cyst Volume in mm^3	Cyst Surface Area in mm^2	Cord Volume[3] in mm^3	Cord Surface Area[4] in mm^2	Lesion Volume[5] in mm^3	Lesion Volume[6] in mm^3
Rat 1	9.2	46.3	1.7	20.2	0.2	9.2	9.4	30.1	1.1	4.3
Rat 7	14.3	62.5	0.9	13.0	0.1	6.9	17.0	38.3	0.9	1.1

1. The values in columns A-F are derived directly from 3-D surface reconstructions.

2. The values in columns G-J are derived from the application of different methods of quantification.

3. Volumes shown are derived from a modification of the elliptical area formula for spinal cord volume used by Blight (1985)

$$V = [(\pi ab) \times h]$$

where a and b are one-half the major and minor axes of the ellipse (cord) and h is the length of the cord segment being measured.

Column G values are not significantly different from those in column A (P = 0.45, paired students' T).

4. Surface areas shown are derived from the formula for an approximation of an elliptical cylinder where

$$S = 2\pi\left[\sqrt{\frac{a^2+b^2}{2}}\right]h + 2\pi ab$$

and a and b are one-half the major and minor axes of the ellipse (cord) and h is the length or height of the spinal cord segment being measured.

The values in column H are not significantly different to those in column B (P = 0.12, paired students' T).

5. The volume of the lesions for each rat were derived from adding all surface area data obtained by 2-D morphometry for serial histological sections x the section thickness. That data (column I) is not significantly different than data in column C (P = 0.5, paired students' T).

6. This volume data is derived from a fustrum model of the spinal cord lesion, after Bresnahan et al. (1991)

$$V = 1/3h[B_1 + B_2 + (B_1 * B_2)^{1/2}]$$

where B_1 and B_2 are the areas of the cone bases, h is the distance between bases, and V is the volume.

The volumes in column J are not significantly different from the data shown in column C (P = 0.45, paired students' T).

* * *

This Table demonstrates our ability to quantitatively query three dimensional reconstructions, allowing comparison to other means of computing spinal cord and/or spinal cord injury surface and volume. Quantitative interrogation of the 3-D reconstructions provide precise surface areas and volumes and were computed using the following equation for a prismatoid, a triangular tiled region between two parallel contours: $V = \frac{h}{6}(B_1 + 4M + B_2)$ where B_1 is the area of the lower base, B_2 is the area of the upper base, M is the area of the midsection joining the bases and h is the separation between contours. With n parallel slices of contours equally spread, the composite volume computation results in: $V1 = \frac{h}{6}(B_1 + 4\sum_{1}^{n-1} Mi + 2\sum_{2}^{n-1} Bi + Bn)$.

Furthermore, this precise evaluation validates other algebraic models used in the literature.

1982). Since our stimulating electrodes are spaced ca. 2 vertebral segments rostral and caudal (and equidistant) from the experimental lesion, one might expect a preferential movement of phagocytes away from the lesion towards the epidural anode. Since the massive accumulations of macrophages are believed to cause more harm to surrounding healthy CNS parenchyma than they prevent during the inflammatory process (Blight 1985), a reduction in their numbers might be considered as a component of the response to applied voltages leading to behavioral recovery (Borgens 1992).

In the annual report of 1996 we stated that: *'"field-- treated animals show a consistent lower macrophage count (on the order of about 5 %) than controls, as well as a reduction in the percent cavitation of spinal cord parenchyma . While our quantitative evaluation and statistical comparisons are not at this time completed , the trends are in the right direction ."*(Page 16, paragraph 1). This trend did not hold up however, following the completion of all animals and a thorough examination of the data. While the negative result was unexpected (and somewhat disappointing), we are confident in the thoroughness of our evaluation, and the reliability of the experimental design. This experiment has been submitted to the Journal of Neurological Sciences for publication, and is now under review .

We will not repeat the methods used in this investigation, but provide the reviewer in the section below, the complete data and statistical evaluation.

Completed Results

Fig 1 shows the mean and standard area per histological section of the macrophage area and macrophage cell count in both experimental and control (sham treated) groups for all 16 animals. Fig 2 further evaluates these data by defining the "lesion" in two different ways used to determine the density of macrophages in the damaged region (macrophage/mm^2 of lesion). In Fig 2 A, the lesion is defined as the total area of macrophage containing, cystic parenchyma of the central lesion -- but not including islands of relatively intact parenchyma contained within this perimeter. In Fig 2 B, the lesion is defined as this same area, however islands of "intact" parenchyma is not excluded from the calculation of lesion area. Fig 3 shows the means and standard errors per histological section of cystic areas in experimental and control groups. Table 2 and Table 3 are summary tables providing the relevant statistical comparison of these data. Note that neither macrophage density or cavitation area is statistically significantly different between the two groups.

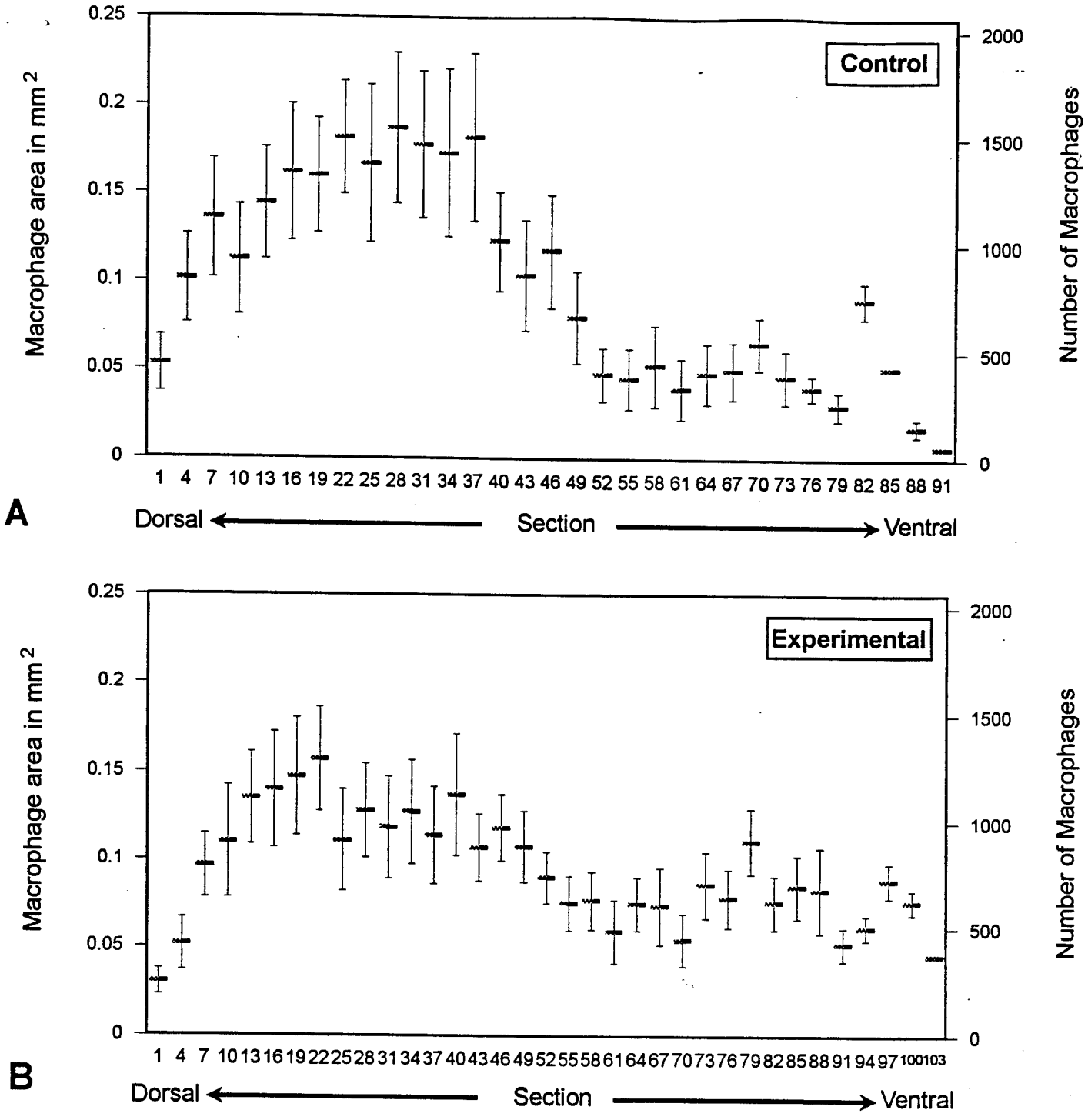

Figure 1 **A** and **B** show the mean and standard error per section of the macrophage area and macrophage count in the control and experimental groups respectively.

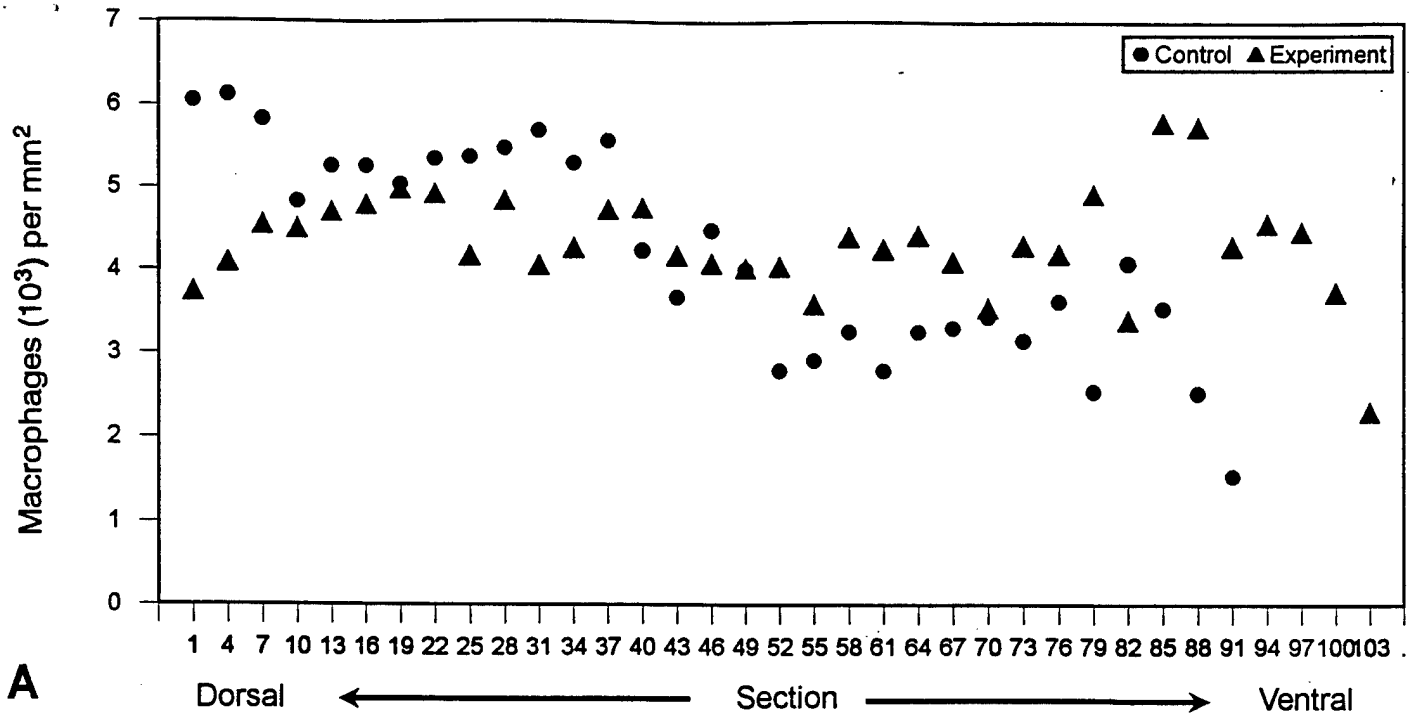

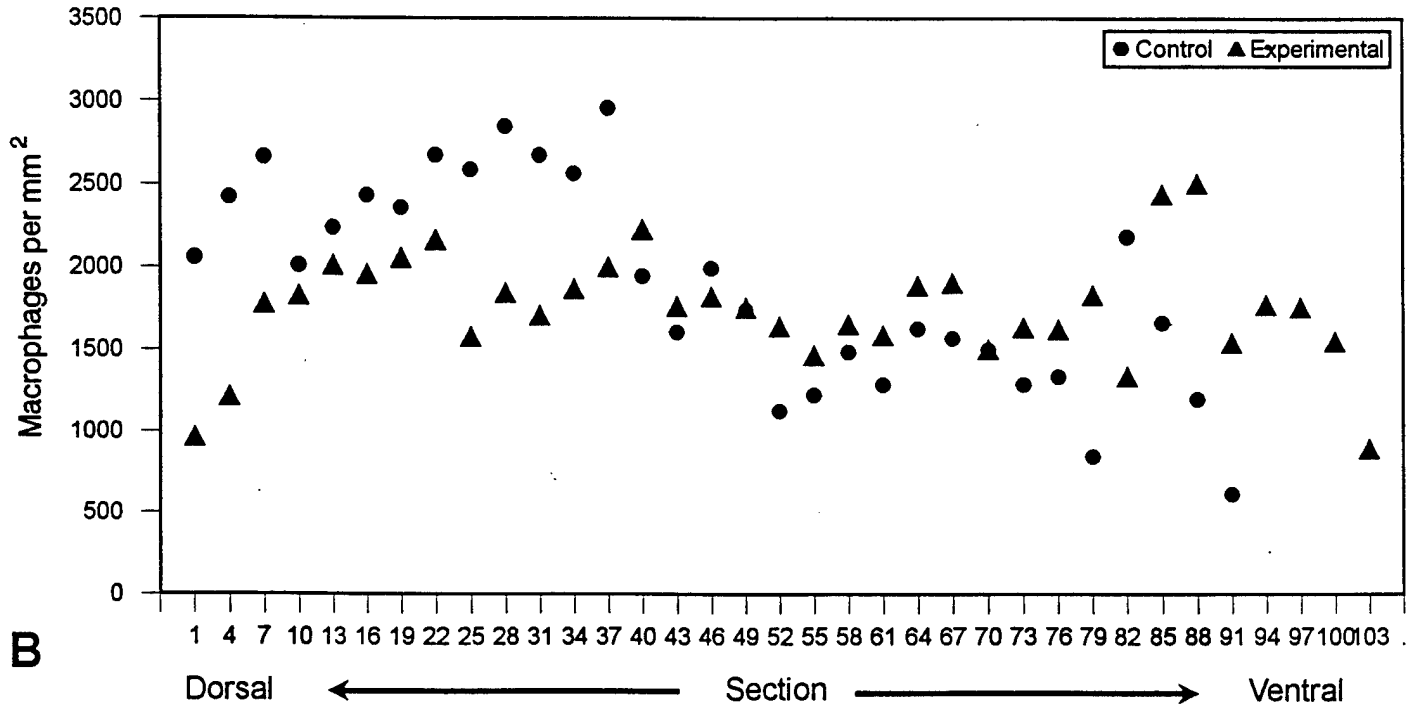

Figure 2 **A** shows the number of macrophages per mm^2 when the lesion is defined as the area composed of macrophages and cysts. **B** shows the number of macrophages per mm^2 when the lesion is defined as above, but also including well stained "intact" parenchyma.

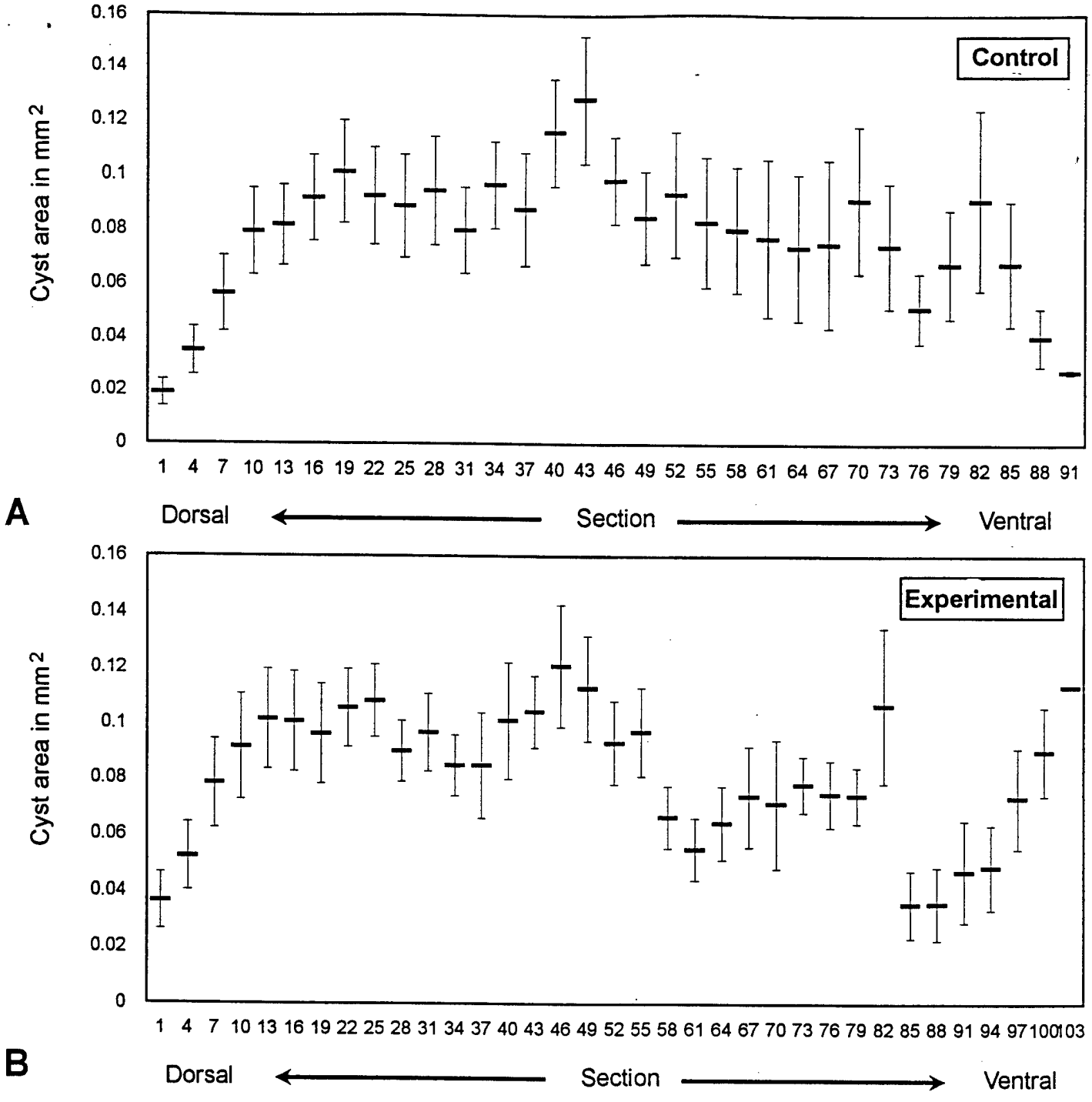

Figure 3 **A** and **B** show the mean and standard error per section of the cystic area in the control and experimental groups respectively.

Table 2 A comparision of control and experimental lesions for all spinal cords

		CONTROL		EXPERIMENTAL		Student's T, unpaired[6]
		N	Mean ± SEM	N	Mean ± SEM	
A	**Lesion[1]** Area (mm^2)	12	9.7 ± 0.9	12	11.1 ± 1.1	P = 0.33
B	**Macrophages** Area (mm^2)[2]	12	2.6 ± 0.5	12	2.4 ± 0.4	P = 0.80
	Percent (%)[4]	12	26.4 ± 3.7	12	22.0 ± 3.0	P = 0.36
C	**Cysts and Cavities** Area (mm^2)[2]	12	1.9 ± 0.3	12	2.1 ± 0.3	P = 0.60
	Percent (%)[4]	12	18.6 ± 2.0	12	18.3 ± 1.3	P = 0.91
D	**Cysts and Macrophages** Area (mm^2)[3]	12	4.4 ± 0.7	12	4.5 ± 0.5	P = 0.96
	Percent (%)[5]	12	45.0 ± 3.8	12	40.2 ± 3.3	P = 0.36

1. Row A shows the mean unit area in mm^2 of the lesion [defined to include macrophage accumulation, cysts, and relatively "intact" parenchyma (see methods)].

2. The unit area in mm^2 of macrophage accumulations (row B) and cavitation (row C) respectively.

3. The unit area in mm^2 of macrophage accumulations and cavitation (row D).

4. The percent of macrophage unit area per unit area of the lesion (row A), and the percent of cystic cavities unit area per unit area of the lesion (row A).

5. Total percent of cavitation and macrophage accumulation unit area per lesion (row A).

6. The statistic used was the two tailed, unpaired student's T: comparing experimental vs. control means. Note there is no significant difference between these groups.

Table 3 Statistical comparison of the mean areas of lesions, macrophages, and cysts per section.

		CONTROL		EXPERIMENTAL		Student's T, unpaired[4]
		N	Mean ± SEM	N	Mean ± SEM	
A	**Lesion[1]** Area (mm^2)	31	0.39 ± 0.02	35	0.43 ± 0.02	P = 0.11
B	**Macrophages** Area (mm^2)[2]	31	0.10 ± 0.01	35	0.09 ± 0.01	P = 0.80
C	**Cysts and Cavities** Area (mm^2)[2]	31	0.08 ± 0.00	35	0.08 ± 0.00	P = 0.56
D	**Cysts and Macrophages** Area (mm^2)[3]	31	0.18 ± 0.01	35	0.18 ± 0.01	P = 0.98

1. Row A shows the mean unit area in mm^2 per section of the lesion, defined to include macrophage accumulations, cysts, and relatively "intact" parenchyma (see methods).

2. The mean unit area per section in mm^2 of macrophage accumulations (row B) and cavitation (row C) respectively.

3. The mean unit area per section in mm^2 of macrophage accumulations and cavitation (row D).

4. Statistic used was the two tailed, unpaired student's T: comparing experimental vs. control section means. Note there is no significant difference between these groups.

3.) Regeneration and Guidance of Spinal Cord Axons into Tubal Fasciculation Pathways by Applied Electric Fields

Background

On page 17 of last years report, we briefly introduced the rationale and preliminary results of an experiment designed to test the combination of an applied electric field with a polymeric guidance channel (fasciculation pathway) to enhance regeneration and guidance of regenerating spinal axons in the adult guinea pig. At that time, 16 control animals (fasciculation tube plus inactive stimulator unit) had been evaluated, but only 6 experimental applications. Over this year, we have completed this experiment with a full compliment of 23 experimental animals in which anterograde tract tracing (with tetramethylrhodamine dextran) was performed -- as well as an additional 10 animals in which retrograde tracing was performed (to clearly demonstrate the origins of nerve fibers found within the fasciculation tube in the experimentals). Since this experiment is now complete, we provide in this report full details of the rationale, procedure, and results. This work is planned to be submitted to the journal Neuroscience later this fall. Most importantly, these data unequivocally support the observation that an extracellular voltage, can not only produce axonal regeneration within the mammalian spinal cord, but likely guide it as well.

There are many choices for investigation of tubal fasciculation pathways to help sustain and direct nerve regrowth. These include: silastic (silicone rubber), poly (DL - lactide -episilon - caprolactone, PLLA/PCL) tubes, polyacrylonitrile/polyvinyl chloride (PAN/PVC) guidance channels, polygalictin and polypropylene mesh tubes, and simple polyethylene guidance tubes, to name only a few. These tubal fasciculation pathways are used in the attempt to extend the gap distance that nerves can regenerate during peripheral fascicular repair, help to align the endoneurial components, strengthen the repair site, and create an environment more conducive to nerve regeneration as well as being more favorable to neuronal support cells. There is little evidence that such tubes alone can rescue the abortive regeneration that naturally occurs following axonal damage in the brain and spinal cord, however.

Our choice of silicone rubber was based on the historically good coaption of this material with nervous system tissues and its electrical insulating capability (Bloch and Hastings, 1982). The latter allow the tube to not only capture and aggregate regenerating axons, but as well permit the use of an inserted (and likewise silicone

rubber insulated), electrode (the cathode), to preferentially draw current into the tube's open bores completing the circuit from an external anode (Fig. 4A). The use of a Silicone adhesive to seal the hole in the center of the tube used to insert the electrode eliminates an alternate current pathway.

It is important to emphasize that in all tests of neurite guidance or axonal regeneration to applied electrical fields under physiological conditions, this response is mediated by the cathode. Axons grow towards cathodes, and away from anodes (Borgens 1992). Indeed, axons or neurites facing the anode undergo marked retrograde degeneration. Therefore, to induce axonal growth towards and into the tubes, a cathode was located within its center. We were unable to test the opposite polarity, however. The electrode products produced by anodes during DC stimulation are quite cytotoxic compared to the antipode, which is relative innocuous at modest levels of direct current (Borgens, 1989). We learned in pilot trials that anodal stimulation within the confines of the tube produced such an unhealthy local environment for cells that early cellular ingrowth, and even subsequent scar tissue plugs did not occur with this polarity of application.

The Implant

The constant current (DC) Implant consisted of two components: the body of the stimulator and a hollow silicone rubber fasciculation pathway -- containing an active negative electrode (cathode) or sham electrode within its center.

The stimulator was identical to a previously reported design (Borgens et al 1986b) using one 3V Lithium Cell (Ray o Vac 1225 BR) connected to a constant current source (National Semiconductor LM 334 Z) which regulates the DC output to be steady, and a 1/8th watt resistor to set the total current to 0.1 μA. Electrodes were constructed of multistrand stainless steel (Cooner Wire, Chatsworth CA) insulated with silicone rubber. Anode electrodes were fashioned from 30 gauge multistrand, and cathodal electrodes from 50 gauge multistrand. The entire unit was potted in beeswax and subsequently, medical grade elastomer (Dow Corning 382). About 3mm of the distal tip of the positive electrode (anode, 14 cm long) was stripped with watchmakers' forceps, and the individual strands of the multistrand wire were splayed out and coiled to provide a relatively large surface area. The distal tip of the cathode, (negative electrode), was stripped of approximately 1 mm of insulation and was inserted into the center of the tube through a small hole made with a 20 gauge needle. The electrode,

Fig.4

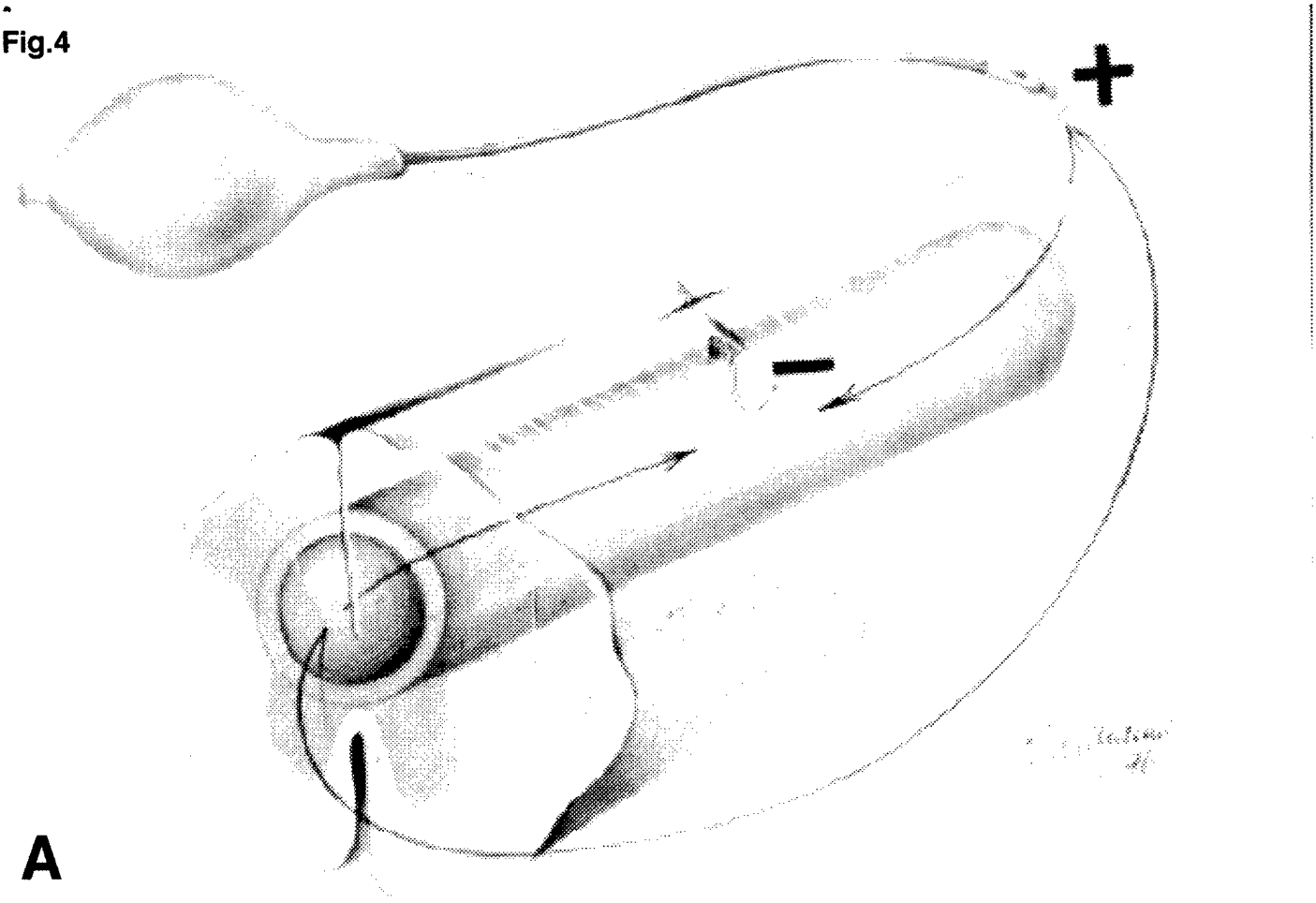

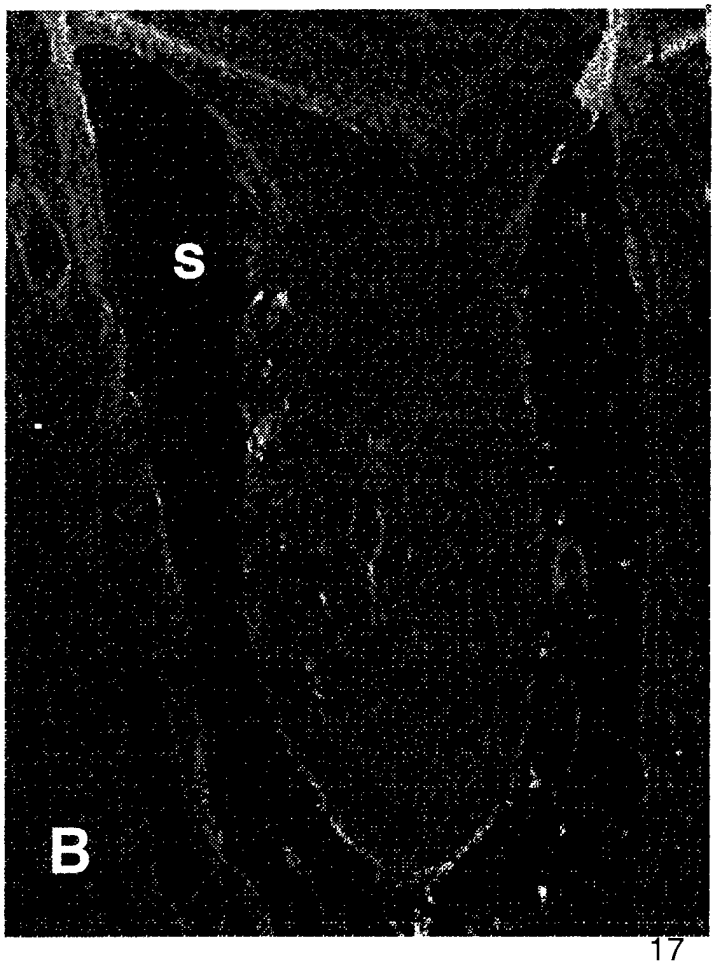

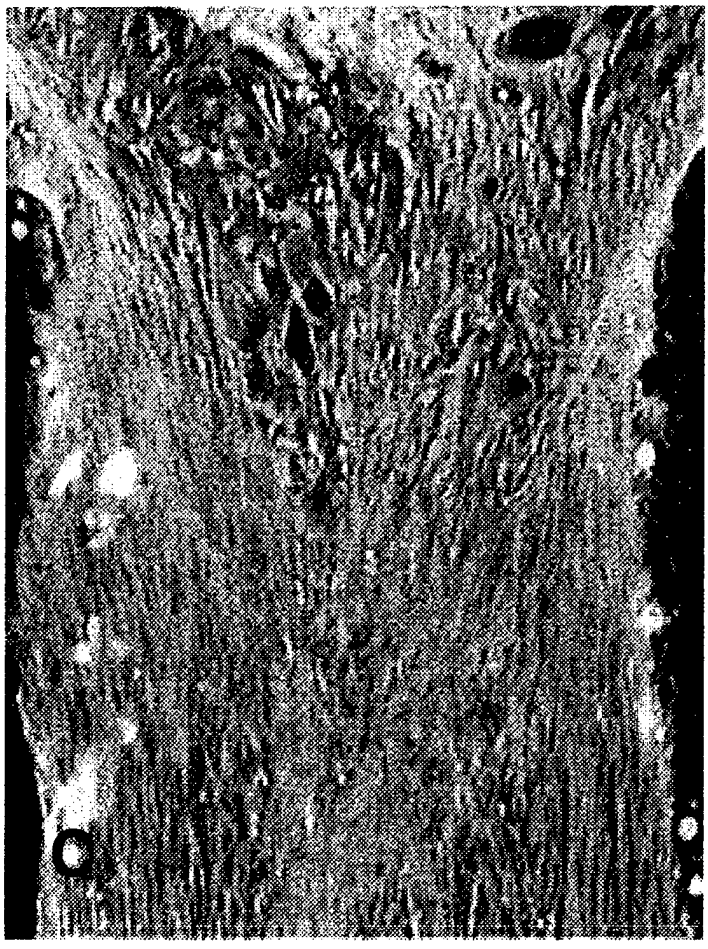

with its uninsulated tip within the center of the tube, was glued in place and the access hole sealed with medical grade silicone based elastomer.

The fasciculation pathway was fashioned from a 6 mm long piece of medical grade silicone rubber tubing (0.94 mm O.D. X 0.51 mm I.D. Dow Corning #602-135). With both ends open, and a centrally located cathode, current could enter both ends to complete the circuit from an externally placed anode (Fig 4A). This would produce an electrical field of approximately 1mV/mm within the tube. The field strength would fall off steeply (approximately the inverse cube of the distance) to a level we estimate [on the basis of previous direct measurement (Borgens et al 1990)] to be about 100-200 μV/mm in the tissues at distance from the tube. With approximately 40 mA/h capacity the units would be functional for about one month. Control or sham units were constructed from non functional components and were physically indistinguishable from active units.

Surgery

Adult female guinea pigs (ca. 500 gm, Hartley strain) were used for these experiments. Anesthesia was performed with an intramuscular injection of a mixture of 60 mg/kg ketamine HCl, and 12 mg xylazine. The dorsal aspect of the spinal cord at a mid thoracic level was exposed by a partial laminectomy. The spinal cord was incised with a fine cutting device (Moria micro blade, 15 degree angle) along its midline for approximately 7 mm, and to the depth of about the central canal. Into this longitudinal fissure the fasciculation tube was inserted, and pushed into the spinal cord such that both ends of the tube were fully pressed into spinal cord parenchyma, with the electrode wire exiting its center exposed at the dorsal surface. Subsequently, the wounds were close in layers. The stimulator body was placed within a subcutaneous fat pad, between the shoulders, approximately 5-7 cm from the spinal cord surgery. The stimulator electrodes were held in place with 3-0 silk suture, the positive electrode located about 1-2 vertebral segments caudal to the placement of the tube, and sutured to paravertebral musculature. The site of the stimulator was closed in layers, and the skin incision closed with wound clips. Twenty Experimental and sixteen Control (or sham treated) Guinea pigs were evaluated at 60 days post implantation of the stimulator and fasciculation tube. Three weeks following implantation, the animals were re anesthetized, and the stimulator was surgically removed by clipping both electrodes.

Anatomical Procedures

Approximately 24 hours before the scheduled sacrifice, animals were anesthetized, and the spinal cord was exposed by a partial laminectomy approximately 2 vertebral segment's rostral, and 2 vertebral segments caudal, to the two ends of the tube. At these two locations, tetramethylrhodamine dextran (*Flouro Ruby*, Molecular Probes, Inc.) was injected into the dorsal half of the cord by previously described techniques (Borgens & Bohnert, 1997). In this way, white matter projections directed towards the open bores of the tube were anterogradely filled allowing spinal long tract tracing. In a second group of animals, long tract tracing was not used. Instead, a retrograde uptake procedure was utilized to help elucidate the cell bodies giving rise to axons that were found to enter the experimental tubes. In this procedure, the dorsal surface of the tube and its electrode exiting it were surgically exposed, the electrode was carefully withdrawn, and crystals of rhodamine dextran were inserted into this hole - into the center of the tube - using the sharp tip of a minutia pin. Immediately following insertion of the dye crystals, a small dab of silicone glue was applied to the hole to seal it. This was allowed to set up "to surface dry" for about 10 minutes prior to closure of the wounds. If care was taken to keep the surgery site relatively dry, this procedure could be carried out with minimal to no leakage of dissolved marker back into the interstitial environment surrounding the tube. In all cases, animals were sacrificed following deep anesthesia with ketamine/xylazine, and perfusion fixed by cardiac puncture with 6 % paraformaldehyde and 0.5 % glutaraldehyde. The spinal cord containing both sham and experimental fasciculation tubes was dissected free for further immersion fixation prior to subsequent anatomical preparation, imbedding in paraffin, and longitudinal horizontal sectioning on a rotary microtome by previously described techniques (Borgens & Bohnert, 1997).

Histological sections were viewed on an Olympus Van Ox Universal microscope. Fluorescent darkfield microscopy utilized several excitation and barrier filter combinations, the most routine used for the rhodamine dextran were 545/790 and 495/475 (Excitation/Barrier filter wavelength in nms). Darkfield images were viewed with an 3 CCD camera and a DEI-750 processor (Optronics, INC.), and acquired to a Macintosh Quadra 800 computer with MediaGrabber soft ware. Color Plates were produced using Colorit and Powerpoint software.

Results

General Procedure and Anatomy

Animals tolerated the procedure well, and the minor mortality was not significantly different between the experimental and control groups. All stimulator units were functional at the time of their removal since the battery was not exhausted for another month of continuous operation. Both ends of the tube were visually confirmed to be imbedded in the parenchyma of the spinal cord at surgery, in 5 cases (4 controls, 1 experimentals), one end worked out of the cord at the dorsal incision allowing evaluation of only one end of the hollow tube. In nearly every case, longitudinal horizontal sections provided a clear definition of where the walls of the silastic tube had been , and the mat of tissue that formed inside. The sections were cut at 15 μm, and the thin sheet of silastic remaining as the "wall" on either side of the tissue plug was lost during tissue processing for histology (Fig 4b). This space is marked "s", as seen in darkfield in Fig. 4b. One week after insertion, conventional histology confirmed that the tips of the hollow tube for a distance of less than 1 mm had filled with mainly blood born elements, and more dense material, probably formed from clotting blood. By one month, this plug of tissue was beginning to become more dense with loose connective tissue, yet still many blood born cellular profiles were visible such as macrophages. By two months, the plug usually extended into the tube for a depth of 1-2 mm on both ends (when both were avalaible for evaluation) and showed a typical appearance of damaged CNS parenchyma that surrounded the implanted tube. Namely, the tube was densely filled with many cellular species, including some peripheral elements such as Schwann cells, and showed both large and small cavitations within the ca. 1-2mm plug of tissue entering the open bores. The implantation of the tube causes enormous damage to the delicate CNS tissues, and the cavitated, cystic, and vascularized "scar" tissue surrounding the tube for a distance of several hundred microns appeared similar to that tissue that intruded into its open ends (Fig. 4c). Though the scar tissue "plug" extended sometimes deeply into the tube, in *no instance* at the sacrifice time used in this study, (2 months), did the complex tissue plug invading the open ends of the tube, meet at its center (see below).

Anterograde Tract Tracing :Control Preparations

Figure 4a & b, shows a typical tissue plug one end of a fasciculation tube containing a sham electrode. Axon profiles were rarely found in the control preparations (2 animals of 16). No axon profiles were observed within this tissue plug (Fig 4b), or in 13 other tubes of the 16 control implantations. In one of these two

exceptional cases, 1-3 axon profiles were observed (one end of the tube only) within the plug of tissue inside the tube. In a second case, one axon was observed to be attached to, and course along the wall of, a small blood vessel penetrating the tube 's interior. We speculate this single fiber was likely autonomic, and not central, in origin. Overall, the *shape* of the tissue penetrating the ends of the silastic tube in control preparations was similar. Like a cork in a wine bottle, the plug usually filled the inside diameter of the hollow tube and was smooth and blunt at its terminal end. This was in stark contrast to the shape of the tissue plugs that formed in over one half of the tube ends of electrically facilitated implantations.

Anterograde Tract Tracing: Electrically Facilitated Implantations

In 12 of 20 experimental tubes, axon profiles were clearly evident coursing throughout the entire length of the scar plug inside the tube (Fig 5b & c). In general, the shape of the plug was more slender and tapered than the scar plug in control cords (Fig.5a, arrow). Fig. 5b & c shows several views of the scar plug shown in Fig. 5a. Note the numerous axons traversing this tissue. In four cases we were able to determine that approximately 10-20 axons penetrated deeply into the plug of scar. In the balance it was impossible to count axons as they were too numerous, and clustered together in columns that intertwined and wound throughout the plug. At the margins, the clarity of individually filled axons showed that they entered the tube from both the outer (dorsal facing) aspect as well as the interior (gray matter facing) aspect. These axons curved abruptly at the mouth of the tube, projecting from cavitated scarified parenchyma surrounding it, and descended into the plug (Fig 6a). Occasionally, tangled masses, or "knots" of fibers formed resembling neuromas, were observed deep within the tissue plug inside the tube.

On the basis of only the anterograde fills, it is likely that the bulk of axons entering the tubes were of spinal long tract origin. Axons of white matter projecting towards the tubes was labeled heavily, and these columns of fibers filled past the margins of the tube. Since the site where the label was injected into the spinal cord was several cm, (two vertebral segments or more) from the mouth of the tube, long and unbranched expanses of well filled fibers were clearly labeled projecting towards the tube. It was difficult to trace individual fibers from these lateral columns through the extremely disrupted terrain of the cavitated and cystic scar tissue that formed around the tube however. Moreover, most, if not all, labeled fibers in and around the implantation site were intensely fluorescent, originating from the injection site - there

Fig 5

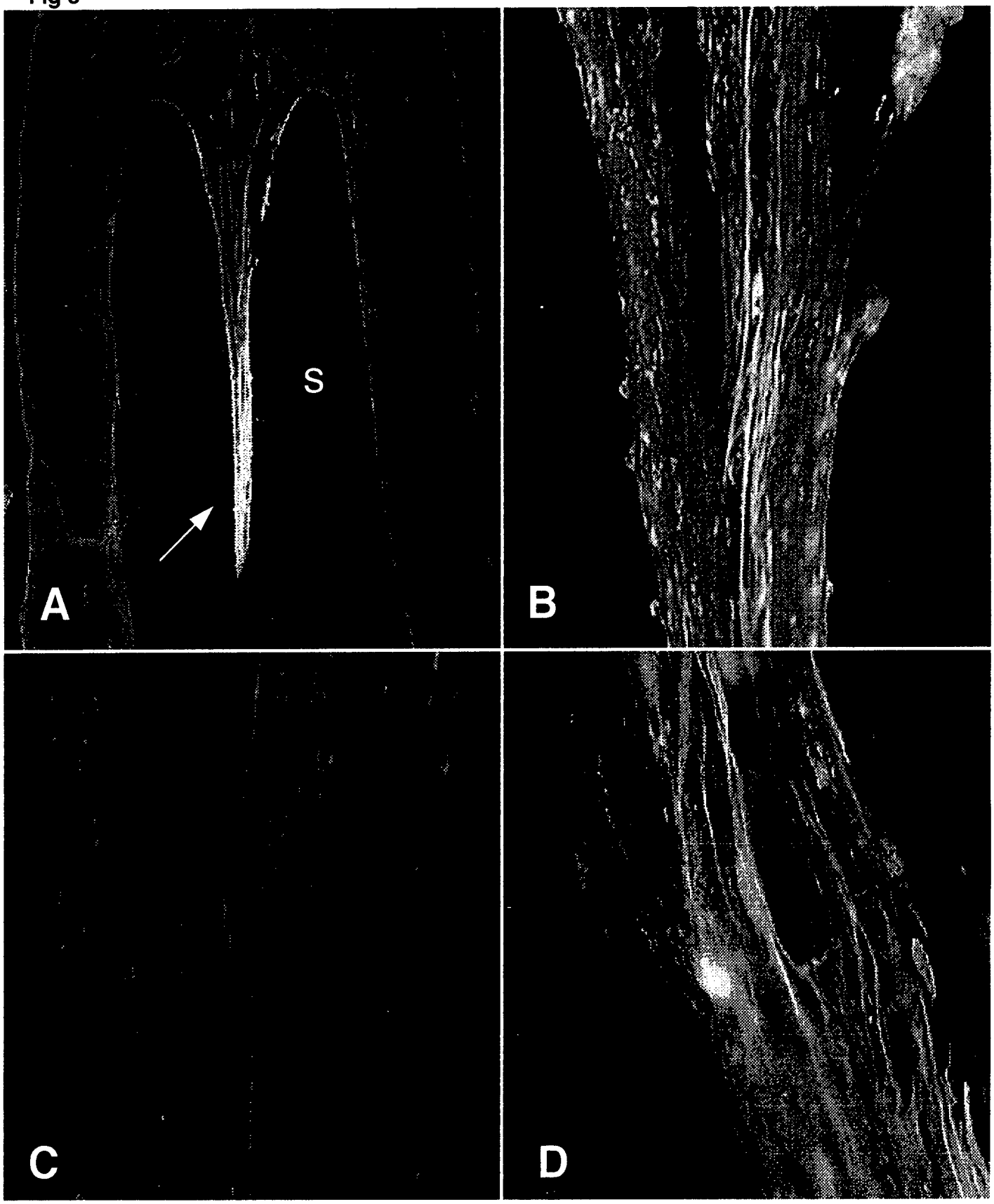

was little evidence of extraneous labeling of axons of peripheral origin, (i.e. dorsal root axons), near the implantation site. This lack of extraneous labeling near the implantation is largely due to the long distance from the site where the label was applied. Overall, we have little evidence for diffusion of label leaking from the injection through the epidural space. Finally, equal numbers of axons entered the open bore of the tube at its medial side -- or said another way -- from deeper gray matter parenchyma. All of these points suggest the greatest numbers of axons within tubes *were of central origin .*

Retrograde Tract Tracing

The retrograde tract tracing experiments were undertaken in response to the large number of axons discovered entering the tubes in which DC current was pulled. Since there was only one case where several axons were found within the control tubes, retrograde studies utilized only *active DC current applications .* This component of our investigation was attempted only to further confirm the origins of axons whose regeneration and guidance was facilitated by the extracellular voltage.

In general, the retrograde procedure worked well, the external margin of the scar tissue plug within the tube was strongly labeled as a variety of cell types at the surface of the cellular plug were exposed to a high concentration of the fluorescent marker confined to the interior of the tube (Fig 6a,b). There was usually no labeling of cells or tissue surrounding the tube as leakage of the dye was minimized by a) insertion of crystals of tetramethylrhodamine dextran (requiring some minutes to become dissolved in insterstial fluid), and b) the immediate sealing of the hole in which the crystals were inserted with elastomer.

Retrograde labeling confirmed that many of the axons within the tube were of central origin. The bulk of labeled fibers were observed to enter the white matter columns adjacent the tube, and remained labeled for variable distances before the intracellular marker became to dilute within axoplasm to reliably mark the extent of projection. It was very evident that such axons made very sharp bends (Fig. 6a), and turns within the scar tissue at the mouth of the tube as they entered the open bore, or made sweeping curved projections to enter the tube at its inside wall, projecting into the tube in close contact with the wall. Though not uncommon, but in much fewer numbers, fibers could be traced into intact gray matter adjacent the medial aspect of the tubes. Moreover, in even fewer numbers intact cell bodies within the gray matter were weakly labeled (Fig. 6c). We were not able to trace an individual axon to be in

Fig 6

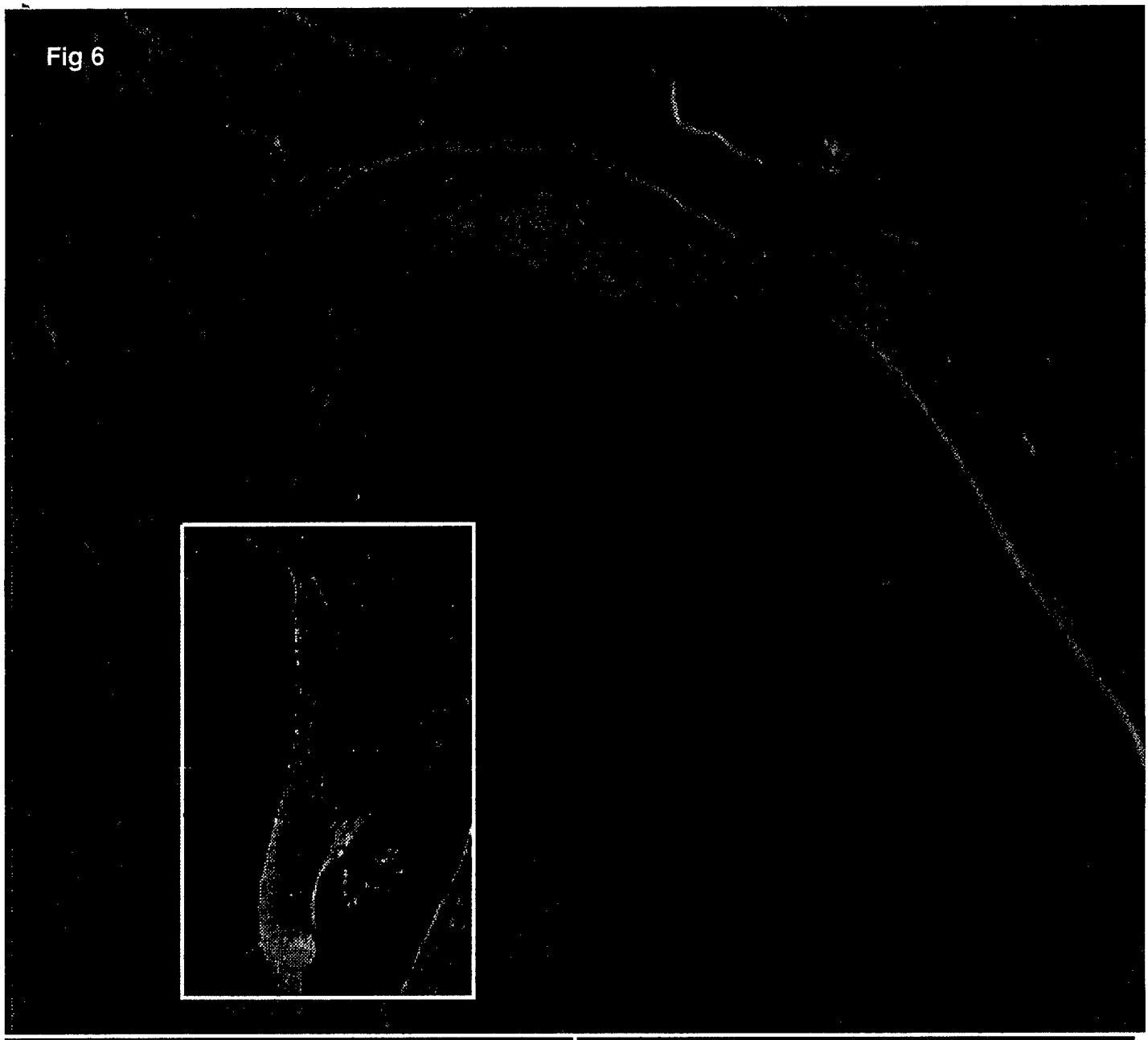

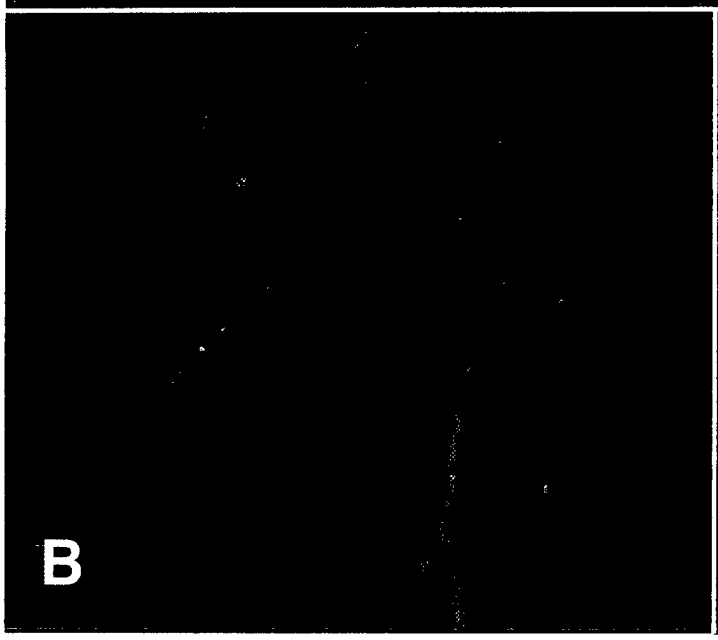

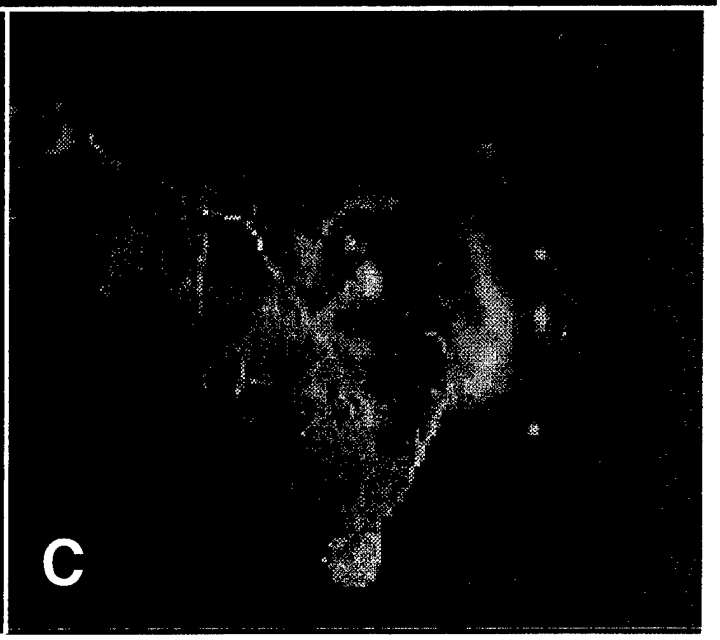

continuity with these labeled cell bodies over this distance of 0.5 - sometimes 1 mm - of extremely disrupted tissue terrain surrounding the implantation site. The presence of such labeled neurons in the pathway of labeled axons, their distance from the implanted tube, coupled to the lack of extraneous labeling adjacent the implant is strong evidence for the central gray matter origin of some axons entering the implant.

4) Fusion and Sealing of Transected or Contused Spinal Cord Axons by Artificial Membrane Surfactants

This experiment has arisen from a recent collaboration with the University of Texas at Austin. Since we are just beginning this ancillary investigation, we provide the reader a brief review. Due to the unanticipated slow recruitment of canine subjects into the clinical trial component of the workplan, (to be completed and detailed in next years report), a one year extension of this contract period was requested and approved. This provides sufficient time to complete and prepare these results for publication.

Background

As previously discussed, damage to the Spinal Cord or Brain produces both immediate and delayed damage to CNS axons. It is this anatomical and physiological compromise that is the biological basis for most of the functional loss. In Spinal Cord Injury, it is clear that most behavioural deficit is due to pathological changes in white matter. Gray matter dissolution is less responsible for the dramatic functional deficits unless contusion or impact occurs directly to the cervical or lumbosacral enlargement (Blight, 1983). It is these surviving white matter projections that have been shown to be the acute targets of applied electric fields that provide trophic and tropic cues for axonal regeneration (Borgens et al 86b, 90, 97). Moreover, substantial, (but variable) numbers of damaged axons go on to separate (proximal segments undergo retrograde degeneration, while distal segments are lost forever through the process of Wallerian degeneration). If one could functionally seal, or fuse, major lesions to axonal membranes (that would normally lead to local dissolution of the nerve fiber) preserving them, than one would be rescuing large numbers of axons for either: 1) other subsequent acute treatments such as the application of electric fields or growth factors, and/or 2) immediate recruitment of some of these fibers back into a pool of conductive fibers mediating behavioural recovery.

In collaboration with Professor George Bittner's group, University of Texas at Austin, we have found that it is indeed possible to do this through the use of specific ion exchange perfusions followed by membrane fusion with the surfactant polyethylene glycol (PEG; 8000-10,000 mw). The most extreme example of such functional axonal membrane fusion would be to completely transect spinal cord white matter -- eliminating *action potential* (AP) conduction along long tracts, fuse the segments following abutment, and then measure a recovery of AP conduction. *We have already achieved this in isolated (organ cultured) adult guinae pig spinal cord as a demonstration of the technique .* It is important to add, that spinal transection is clinically rare, even in severe wartime injuries. Clinical Injuries are blunt force, contusive, traumas leading to marked vascular and ionic imbalance, and eventual gray and white matter loss local to the area of impact. It would be more important in the clinic to be able to fuse major"holes" or lesions in the axolemmas of fibers at the impact zone -- to rescue them from eventual dissolution. This can be accomplished from a technique that could be first shown to be able to join, and functionally fuse, completely separated axon segments.

Methods

Preparing the Spinal Cord

Large Adult Guinae pigs are deeply anesthetized with Ketamine / Xylazine, and immediately perfused with a lactated *Krebs solution* by cardiac puncture. The spinal cord in its near entirety (cervical to sacral) is dissected free and immersed in cold oxygenated Krebs. The spinal cord is longitudinally bisected, or sometimes quartered into the 4 major funnuculei, and these strips placed into a special recording chamber. This double sucrose gap recording chamber has been recently reported (Shi and Blight, 1996), and a brief summary of its design is provided in Fig 7. This chamber provides superior signal to noise ratio for the measurement and recording of compound APs, and allows the simultaneous measurement of compound membrane potential as well (Shi and Blight 1996). In short, this new procedure allows electrical recordings with the "clean" character of intracellular recordings. White matter strips can be maintained in the chamber for up to 40 hours of continuous recording at room temperature.

Fig 7

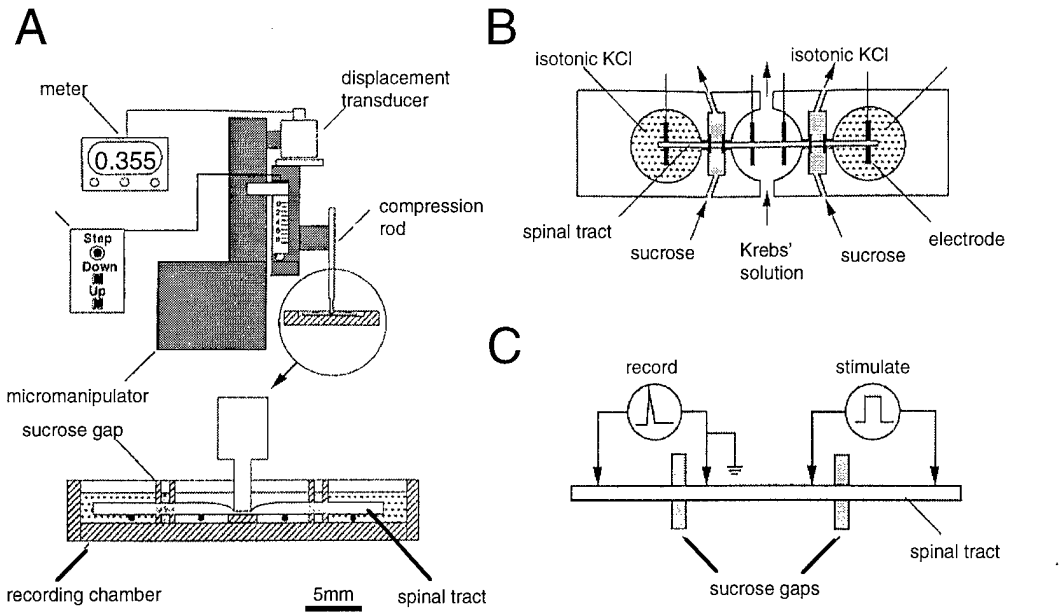

Diagram showing the injury and recording apparatus. *A*: injuries can produced by compression with a Plexiglass rod advanced in the vertical axis with a micromanipulator. The movements of the rod are monitored with a displacement transducer and activated with a stepper motor control. *B*: recording arrangement. The isolated spinal tract is shown mounted in the apparatus, with the injury site placed in the middle of the central well, which is continuously perfused with oxygenated Krebs solution. The two ends of the tract were placed in separate wells filled with isotonic KCl, divided from the central well by narrow channels filled with flowing isotonic sucrose solution. *C*: electrical stimulating and recording arrangement, shown in a scaled diagram. Action potentials were generated at the right sucrose gap, conducted through the injured part of the spinal cord, and recorded at the left gap with the use of a bridge amplifier.

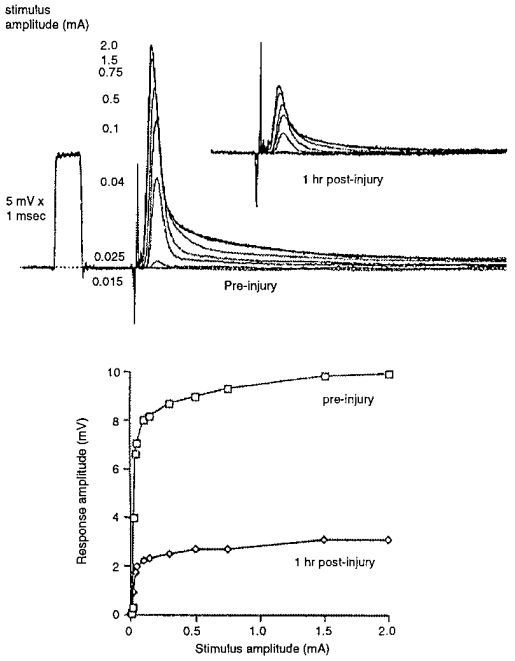

Examination of the relation between stimulus and response amplitude before and after injury, shown (A) in the form of superimposed recordings and (B) as a graphic plot. The compound potential amplitude increased rapidly to a maximum within a narrow range of stimulus intensity between 20 and 200 μA. Above that intensity there was only a slight further increase in amplitude, which was accompanied by decreased conduction delay and increased synchrony of activation. This combination of changes at higher stimulus strengths is consistent with increased current spread, not increased recruitment of nerve fibers. The decrease in amplitude of the compound potential occurred consistently at all stimulus intensities.

from Shi and Blight (1996)

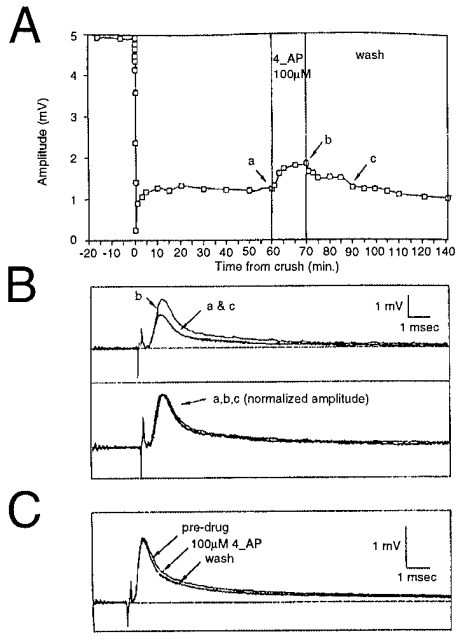

A: plot of compund potential amplitude change with time post-injury, showing the initial loss and recovery, and also the effect of superfusion with 100 μM 4-aminopyridine (4-AP) during the plateau phase. The amplitude increased within 15 min to a new plateau level almost 50% larger than before application. This increase was reversed by wash with normal Krebs solution. *B*: superimposed traces in the *top panel* show the increase in compund potential amplitude with 4-AP and its complete reversal with 20 min of washing. In the *bottom panel* the same traces are plotted, normalized for peak amplitude, to show the absence of any significant change in waveform accompanying the increase in amplitude with 4-AP. *C*: comparable experiment with uninjured spinal cord, the superimposed traces (with a single vertical scale) showing the lack of effect of 4-AP on compound potential amplitude at this concentration, despite a small change in the amplitude of the depolarizing afterpotential.

Fusion Procedure

Following a full characterization of the physiological functioning of the ca. 6 cm spinal cord strip, it is then completely transected, (transversly), at its center within the recording chamber using a microknife. After the loss of conduction is documented by further electrophysiological recording, the fusion procedure is begun. First, cytoplasmic degradation by calcium dependent processes is retarded with a perfusion (for 3 - 5 minutes) of Krebs in which Ca^{++} is replaced with Magnesium, and EGTA is included. This has been shown to markedly retard dissolution of the axoplasm at the cut, (Todd et al, 1990). Secondly, a similar perfusion follows that is hypotonic, (in Na^{+} concentration), by about 50 %. This osmotically swells the ends of severed axons into a "trumpet shape" that facilitates the abutment of proximal and distal segments. During this procedure, a specially fabricated "jig" is used to push the severed segments of cord into very close abutment while a perfusion of PEG is begun to fuse those membranes in close opposition. This is continued for about 5 minutes while square wave stimulation of the cord strip is begun again. If there is no evidence of restored AP conduction, a second attempt is begun. Since PEG has both the property to fuse -- or dissolve cell membranes, only one "second"attempt at fusion is attempted. Any recovering AP is thoroughly documented and evaluated electrophysiologically (conduction velocity, latency, after potential, area under the AP curve etc.).

Anatomical Techniques

To demonstrate an anatomical basis for AP conduction, (ie, fusion of proximal and distal segments): a double label tract tracing is performed on the spinal cord strip in isolation at the end of the regimen of recording. One µl of a flourescent tract tracer, tetramethylrhodamine dextran, is injected 1-2 cm from the fusion site on one segment of spinal cord, while another similar injection of FITC conjugated dextran is performed in the adjacent section. Since only one combination of excitation and barrier filter will reveal the individual dyes, they can be discriminated one from the other. FITC dextran fibers in the rhodamine injected segment would be evidence for anatomical continuity across the fusion site, and visa versa. We have not been able to obtain a proprietary PEG hydrogel for use as a second PEG perfusion This hydrogel is activated by UV light, hardening around the fused membranes and structurally preserving the fusion. In such a case, we could image the exact region of the fusion, without resorting to

inference based on the double label technique. We hope to provide such data before the end of the year.

Preliminary Results

Electrophysiology

We have attempted fusion on over 30 spinal cords in isolation since June, 1996. Our success rate has climbed steadily as we have altered and experimented with the various procedures used during the fusion process. We still do not feel we have an optimum procedure, though our last 15 attempts were all effective. Usually, AP conduction is recovered approximately 5-30 minutes following the initiation of the fusion. The recovered compound AP is reduced in amplitude (15 - 30 % of the original), and usually changes in character over one hour of subsequent recording. This change is usually seen as a slow increase in AP amplitude, and a reduction in the AP duration. We have undertaken 12 control experiments. In 6 cords, electrical recording was continued while the exact procedure used for fusion was carried out , however no PEG was applied. In 6 more control preparations, PEG was applied to incompletely abutted -- but closely opposed -- spinal cord segments. No recovery of AP conduction was observed in controls. Figure 8A shows the original compound AP traversing the untransected strip of cord. Figure 8B shows the loss of the AP following complete transection of the spinal cord. Figure 8C shows the recovered compound AP following PEG fusion. Finally, "D" shows the loss of the recovered AP following retransection through the fused region.

We have used the double label anatomical procedure on only our last successful fusion, and on 6 control preparations. There was no crossing over, or artifactual staining of the inappropriate segment of cord in any control preparation. We believe this is due to the continuous perfusion of the spinal cord with oxygenated Krebs solution during the entire procedure, eliminating the chance that dye leakage from one injection site can contaminate the adjacent spinal cord segment. Our one evaluation of fusion anatomy was only partially successful. The FITC dextran injection failed to mark many fibers, thus few labeled to the transection plane in that segment of cord. The rhodamine dextran injection was very successful, labeling many axons, one column of which was found well labeled in the FITC segment. This is preliminary evidence for the anatomical integrity of transected, but fused, axonal segments.

Fig 8

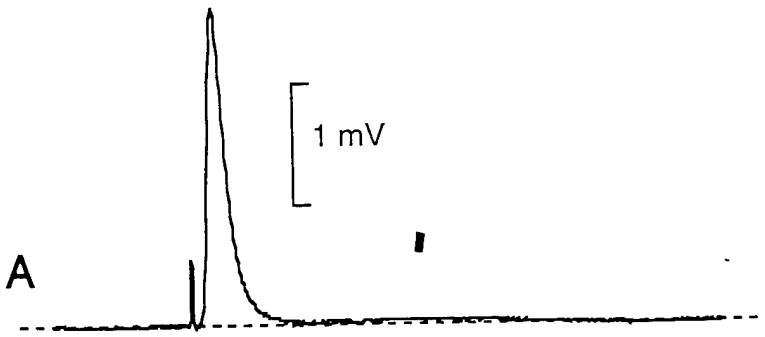

Normal Compound Action Potential
pre cut

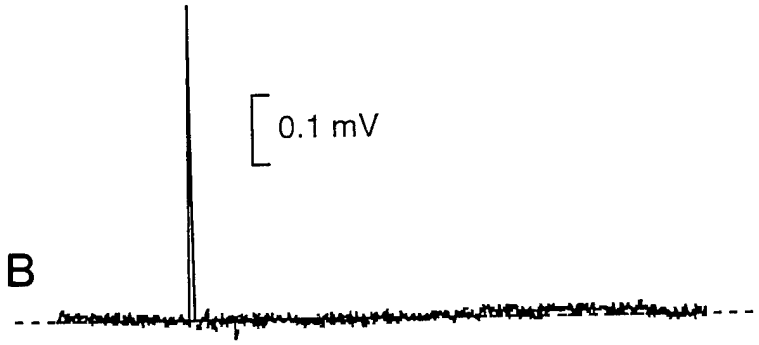

2 min. post cut

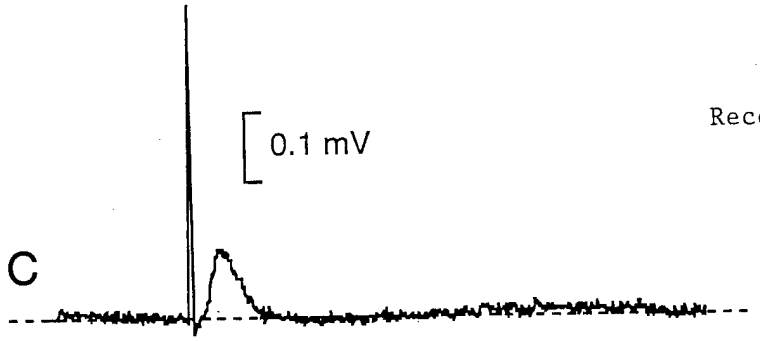

Recovering Compound Potential - post FUSION
50 min.post cut

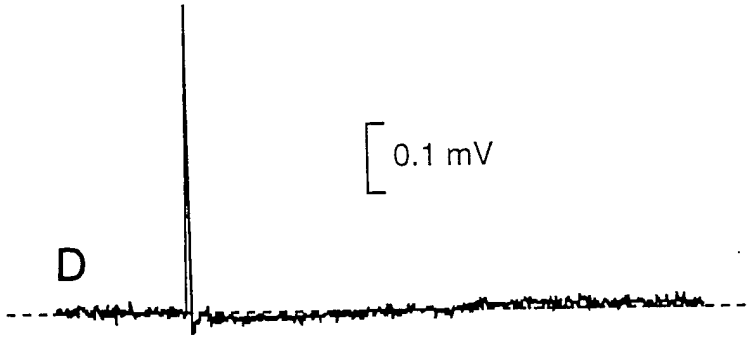

retransection

III. Conclusions

1. In this contract year, we have expanded our development of novel, computer assisted three dimensional surface reconstruction and volume visualization techniques to include precise quantification of pathological structures, as applied to spinal trauma. We noted the general importance of this advancement in the conclusions listed in last years annual report, and this year have fully realized this capability. These data have been accepted for publication by the Journal of Neurological Sciences.

2. Though preliminary examination of data was encouraging, we have now determined that the fully activated macrophage is not a direct target of the applied voltage gradient in spinal cord injury. The density of these phagocytes, and the cavitation of parenchyma associated with them, are not stastically different between experimental and control (sham treated) groups. Thus, we are now less enthusiastic with our notion that the applied voltage gradient enhances behavioral recovery from spinal trauma through a reduction in the cell mediated destructive consequences of the inflammatory response.

3.) Combining the application of a weak extracellular voltage with a surgically implanted "guidance channel" or "fasciculation pathway", clearly induces a striking and robust regeneration of spinal axons for long distances in vivo. This experiment not only demonstrates the trophic and tropic cues provided by imposed electrical fields, but provides a less ambiguous means to determine the optimal field strength required to induce CNS long tract regeneration.

4.) Any restorative method applied to acute and severe nerve trauma must have some degree of surviving nerve processes to be effective. The initial insult leads to further dissolution of the proximal nerve fiber segment (that in continuity with the cell body), and complete loss of the distal segment by Wallerian degeneration. This process can be arrested through a specific regimen of perfusions of the injury site with low ionic Ca^{++}: followed by hypotonic media, and then the application of a molecular surfactant that acts as a synthetic, self organizing membrane fusing proximal and distal

segments. Such a technique has now been shown to be capable of producing functional reconnection of transected spinal axons.

IV. REFERENCES

1. Bajaj C., Coyle C. and Lin K. (1996) Arbitrary topology shape reconstruction from planar cross sections, *Graphical Models and Image Processing* 58, 6: 190-211.

2. Blight, A.R. (1983) Cellular morphology of chronic spinal cord injury in the cat: analysis of myelinated axons by line sampling. *Neuroscience.* 2:521-543.

3. Blight, A.R. (1985) Delayed demyelination and macrophage invasion: A candidate for secondary cell damage in spinal cord injury, Central Nervous System Trauma 2:299-315.

4. Blight A.R., E. Carwile Leroy, Jr., M.P. Heyes. (1997) Quinolinic acid accumulation in injured spinal cord: time course, distribution, and species differences between rat and guinea pig. *J. Neurotrauma* 14, 89-98.

5. Bloch, B., and G. W., Hastings *Plastic Materials in Surgery,* C.C. Thomas, Pub. Springfield, IL (1972)

6. Borgens, R.B. and C.D. McCaig (1989) Artificially controlling axonal regeneration and development by applied electric fields. In: *Electric Fields in Vertebrate Repair.* Co-authored by R.B. Borgens, K.R. Robinson, J.W. Vanable, Jr., and M.E. McGinnis. (Alan R. Liss, New York), Chapter 4. pp. 117-170.

7. Borgens, R.B. (1992) Applied Voltages in Spinal Cord Reconstruction: History, Strategies, and Behavourial Models. In *Spinal Cord Dysfunction, Volume III: Functional Stimulation.* L.S. Illis, Ed., (Oxford Medical Publications, Oxford) Chapter 5 pp. 110-145.

8. Borgens, R.B., A.R. Blight, and D.J. Murphy (1986a) Axonal regeneration in spinal cord injury: A Perspective and new technique. J. Comp. Neurol. 250:157-167.

9. Borgens, R.B., A.R. Blight, D.J. Murphy, and L. Stewart (1986b). Transected dorsal column axons within the guinea pig spinal cord regenerate in the presence of an applied electric field. *J. Comp. Neurol. 250*:168-180.

10. Borgens, R.B., A.R. Blight, and M.E. McGinnis (1987) Behavioral recovery induced by applied electric fields after spinal cord hemisection in guinea pig. Science 238:366-369.

11. Borgens, R.B. , A.R. Blight, and M.E. McGinnis (1990) Functional recovery after spinal cord hemisection in guinea pigs: The effects of applied electric fields. *J. Comp. Neurol.* 296:634-653.

12. Borgens, R.B., J.P. Toombs, A.R. Blight, M.S. Bauer, W.R. Widmer and J.R Cook. (1993) Effects of applied electric fields on clinical cases of complete paraplegia in dogs. J. *Restorative Neurology and Neuroscience* , 5:305-322.

13. Borgens, R.B., D.M. Bohnert (1997) The Responses of Mammalian Spinal Axons to an Applied DC Voltage Gradient *Experiemental Neurology,* 145:376-389.

14. Bresnahan, J.C., M.S. Beattie, B.T. Stokes, and K.M. Conway (1991) Three-dimensional computer-assisted analysis of graded contusion lesions in the spinal cord of the rat. *Journal of Neurotrauma* 8:91-97.

15. Orida, N. and J.D. Feldman (1982) Directional protrusive pseudopodial activity and motility in macrophages induced by extracellular electric fields. *Cell Motility 2*:243-255.

16. Krause, T.L., G.D. Bittner (1990) Rapid Morphological Fusion of Severed Myelinated Axons by Polyethylene Glycol. *Proc. Natl. Acad. Sci. USA,* Vol. 87, pp. 1471-1475.